Fire-related tree cover loss and the Hansen–Fra discrepancy in the Amazon basin (2015–2023): implications for SDG forest monitoring

Pérdida de cobertura arbórea relacionada con incendios y la discrepancia Hansen-Fra en la cuenca amazónica (2015-2023): implicaciones para el monitoreo forestal de los ODS

Perda de cobertura arbórea relacionada a incêndios e a discrepância de Hansen-Fra na bacia amazônica (2015-2023): implicações para o monitoramento florestal dos ODS.

Adilson Celimar Dalmora[a],Andreas Hasse[b], Sinara da Silva Bianchi[c]

a REMIAGRO ENGENHARIA, Travessa Gabriel Afonso 76, Tupinamba, Cachoeira do Sul –RS, (Brasil). 96.506-810 (adilsondalmora@hotmail.com)

b HRES Development GmbH. Erst-Bode-Straße 7, 27432 Bremervörde, Germany.

c Universidade Federal do Rio Grande do Sul (UFRGS), Programa de Pós-Graduação em Engenharia de Minas, (Metalurgia e de Materiais PPG3M), Av. Bento Gonçalves, Porto Alegre - RS, 90650-001 (Brasil).

**Corresponding author: Adilson Celimar Dalmora, email: adilsondalmora@hotmail.com*

To reference this article:
Dalmora et al. (2025). Fire-related tree cover loss and the Hansen–Fra discrepancy in the Amazon basin (2015–2023): implications for SDG forest monitoring. LADEE, 6 (2), 15–60. https://doi.org/10.17981/ladee.06.02.2025.2

Keywords: Amazon, forest disturbance, tree-cover loss, active fire detections, VIIRS, Hansen Global Forest Change, FAO FRA, protected areas, discrepancy ratio, fixed-effects panel.

Palabras clave: Amazonía, perturbación forestal, pérdida de cobertura arbórea, detecciones de incendios activos, VIIRS, Hansen Global Forest Change, FAO FRA, áreas protegidas, razón de discrepancia, panel de efectos fijos.

Palavras-chave: Amazônia, perturbação florestal, perda de cobertura arbórea, detecção de incêndios ativos, VIIRS, Hansen Global Forest Change, FAO FRA, áreas protegidas, taxa de discrepância, painel de efeitos fixos.

Abstract

Forest disturbance related to fires has increased in many regions; however, the extent to which annual fire activity explains the recent loss of tree cover in the Amazon basin and in South American forest systems in general remains insufficiently quantified. This study constructs a harmonized country-year panel for twelve South American countries for the period 2015–2023. The panel includes twelve countries influenced by the Amazon basin (Argentina, Bolivia, Brazil, Chile, Colombia, Ecuador, Guyana, Paraguay, Peru, Suriname, Uruguay, and Venezuela) to capture regional forest dynamics in adjacent biomes. The dataset integrates tree cover loss derived from Landsat, active fire detections from VIIRS, protected area boundaries, interpolated FAO forest area statistics, and macroeconomic indicators. During the study period, the region experienced approximately 45.2 million hectares of cumulative tree cover loss, with Brazil registering the largest share, accounting for over 7.2 million VIIRS fire detections in forest pixels. Forest loss is quantified using a 30% forest cover threshold and analyzed using a fixed-effects panel regression to assess the relationship between fire activity, economic structure, and annual forest disturbance. Year-to-year variations in VIIRS fire detections are closely related to forest cover loss, with an estimated elasticity of loss with respect to fire of approximately 0.22 percent across model variants and forest cover thresholds. A discrepancy index comparing Hansen's gross forest cover loss with the net change in forest area from the FAO Forest Resources Assessment (FRA) indicates that a substantial portion of canopy disturbance is not reflected in national forest statistics. Average discrepancy indices approach 20 in some countries and exceed 40 in extreme annual cases, suggesting that degradation and temporary disturbance are underrepresented in land-use-based reports. Loss within protected areas is also significant, particularly in Venezuela, where approximately 45% of total forest cover loss occurs within protected boundaries. These findings highlight the growing role of fire as a proximate driver of forest disturbance and underscore the need to integrate satellite-based disturbance monitoring with national inventories and socioeconomic data to improve assessments of forest dynamics and progress toward Sustainable Development Goals 13 and 15.

Resumen

La perturbación forestal relacionada con los incendios ha aumentado en muchas regiones; sin embargo, el grado en que la actividad anual de incendios explica la reciente pérdida de cobertura arbórea en la cuenca amazónica y en los sistemas forestales sudamericanos en general sigue sin estar suficientemente cuantificado. Este estudio construye un panel armonizado de país-año para doce países sudamericanos para el período 2015-2023. El panel incluye doce países influenciados por la cuenca amazónica (Argentina, Bolivia, Brasil, Chile, Colombia, Ecuador, Guyana, Paraguay, Perú, Surinam, Uruguay y Venezuela) para capturar la dinámica forestal regional en biomas adyacentes. El conjunto de datos integra la pérdida de cobertura arbórea derivada de Landsat, las detecciones de incendios activos de VIIRS, los límites de áreas protegidas, las estadísticas interpoladas del área forestal de la FAO e indicadores macroeconómicos. Durante el período de estudio, la región experimentó aproximadamente 45,2 millones de hectáreas de pérdida acumulada de cobertura arbórea, siendo Brasil el que registró la mayor proporción, representando más de 7,2 millones de detecciones de incendios VIIRS en píxeles forestales. La pérdida de bosque se cuantifica utilizando un umbral de cobertura forestal del 30% y se analiza mediante una regresión de panel de efectos fijos para evaluar la relación entre la actividad de incendios, la estructura económica y la perturbación forestal anual. Las variaciones interanuales en las detecciones de incendios VIIRS están estrechamente relacionadas con la pérdida de cobertura forestal, con una elasticidad estimada de la pérdida con respecto al fuego de aproximadamente el 0,22 por ciento en las variantes del modelo y los umbrales de cobertura forestal. Un índice de discrepancia que compara la pérdida bruta de cobertura forestal de Hansen con el cambio neto en el área forestal de la Evaluación de los Recursos Forestales (FRA) de la FAO indica que una parte sustancial de la perturbación del dosel no se refleja en las estadísticas forestales nacionales. Los índices de discrepancia promedio se acercan a 20 en algunos países y superan 40 en casos anuales extremos, lo que sugiere que la degradación y la perturbación temporal están subrepresentadas en los informes basados en el uso de la tierra. La pérdida dentro de las áreas protegidas también es significativa, particularmente en Venezuela, donde aproximadamente el 45% de la pérdida total de cobertura forestal ocurre dentro de los límites protegidos. Estos hallazgos resaltan el papel cada vez mayor del fuego como un factor próximo de perturbación de los bosques y subrayan la necesidad de integrar el monitoreo satelital de perturbaciones con los inventarios nacionales y los datos socioeconómicos para mejorar las evaluaciones de la dinámica forestal y el progreso hacia los Objetivos de Desarrollo Sostenible 13 y 15.

Resumo

A perturbação florestal relacionada a incêndios aumentou em muitas regiões; no entanto, a extensão em que a atividade anual de incêndios explica a recente perda de cobertura arbórea na bacia amazônica e nos ecossistemas florestais sul-americanos em geral permanece insuficientemente quantificada. Este estudo constrói um painel harmonizado país-ano para doze países sul-americanos no período de 2015 a 2023. O painel inclui doze países influenciados pela bacia amazônica (Argentina, Bolívia, Brasil, Chile, Colômbia, Equador, Guiana, Paraguai, Peru, Suriname, Uruguai e Venezuela) para capturar a dinâmica florestal regional em biomas adjacentes. O conjunto de dados integra a perda de cobertura arbórea derivada de imagens Landsat, detecções de incêndios ativos pelo VIIRS, limites de áreas protegidas, estatísticas interpoladas de área florestal da FAO e indicadores macroeconômicos. Durante o período do estudo, a região apresentou uma perda cumulativa de cobertura arbórea de aproximadamente 45,2 milhões de hectares, com o Brasil registrando a maior parcela, respondendo por mais de 7,2 milhões de detecções de incêndios em pixels florestais do VIIRS. A perda florestal é quantificada utilizando um limiar de cobertura florestal de 30% e analisada por meio de uma regressão de painel com efeitos fixos para avaliar a relação entre a atividade de incêndios, a estrutura econômica e a perturbação florestal anual. As variações anuais nas detecções de incêndios pelo VIIRS estão intimamente relacionadas à perda de cobertura florestal, com uma elasticidade estimada da perda em relação ao fogo de aproximadamente 0,22% entre as variantes do modelo e os limiares de cobertura florestal. Um índice de discrepância que compara a perda bruta de cobertura florestal de Hansen com a variação líquida da área florestal da Avaliação de Recursos Florestais (FRA) da FAO indica que uma parcela substancial da perturbação da copa não é refletida nas estatísticas florestais nacionais. Os índices médios de discrepância se aproximam de 20 em alguns países e ultrapassam 40 em casos anuais extremos, sugerindo que a degradação e a perturbação temporária são sub-representadas em relatórios baseados no uso da terra. A perda dentro de áreas protegidas também é significativa, particularmente na Venezuela, onde aproximadamente 45% da perda total de cobertura florestal ocorre dentro dos limites de áreas protegidas. Essas descobertas destacam o papel crescente do fogo como um fator imediato de perturbação florestal e ressaltam a necessidade de integrar o monitoramento de perturbações baseado em satélite com inventários nacionais e dados socioeconômicos para melhorar as avaliações da dinâmica florestal e o progresso em direção aos Objetivos de Desenvolvimento Sustentável 13 e 15.

DOI: 10.17981/ladee.06.02.2025.2

Date received 01/12/2025.
Date of acceptance 31/12/2025.

© The author; licensee Universidad de la Costa - CUC.
LADEE vol. 6 no. 2, pp. 15–33. July- December, 2025
Barranquilla. e-ISSN 2744-9750 (On line)

1. Introduction

Tropical and subtropical forests in South America play a central role in the global carbon cycle, regional climate regulation, and biodiversity conservation. The Amazon basin and adjacent biomes store large stocks of aboveground biomass, provide moisture recycling that supports rainfall patterns across the continent, and sustain a wide range of ecosystem services for local and distant populations. Over the past several decades, however, these forests have come under increasing pressure from a combination of land-use change, infrastructure expansion, and climate variability. Satellite-based analyses have documented extensive forest loss in the humid tropics since the early 2000s, with the Amazon basin emerging as one of the most affected regions (Hansen et al., 2013; Achard et al., 2002). At the same time, national forest inventories and land-use statistics often present a more moderate picture, highlighting both definitional differences and gaps in the monitoring of degradation and temporary disturbance (Li et al., 2017; Egusa et al., 2020).

Fire has become an increasingly important component of this transformation. Recent work based on global Landsat-derived forest disturbance and VIIRS active fire detections shows that forest disturbance due to fire reached unprecedented levels in 2023 and 2024, with the largest increases in intact forest landscapes and tropical domains (Potapov et al., 2025; Tyukavina et al., 2015). The share of fire-related disturbance in total forest loss has increased compared with the early 2000s, and fire emissions from forests have risen where disturbance affects high-biomass tropical forests (Baccini et al., 2017; Maxwell et al., 2019). In South America, extreme fire years such as 2016, 2019, and 2020 have affected both long-established agricultural frontiers and more remote forests, generating visible smoke plumes, air-quality impacts, and renewed policy debate about the resilience of Amazonian and adjacent forest systems. Examples of large fire events and associated smoke plumes observed by satellite imagery during the study period are illustrated in Figure 1.

Figure 1. Satellite imagery of major fire events in Brazil and Bolivia in 2019 and in the Pantanal in 2020, illustrating the spatial extent of smoke plumes and burn scars associated with large fire seasons in the study period.

The drivers of these fire dynamics are multiple. Land-use practices in the region often rely on fire to clear land, manage pasture, and maintain shifting cultivation systems, and the expansion of road networks, mining operations, and large-scale agriculture has increased the likelihood that such fires escape into surrounding forests (Sonter et al., 2017; Moffette & Gibbs, 2021; Amaral et al., 2021). At the same time, climate change has altered the frequency and intensity of fire-conducive weather, lengthened dry seasons and increasing fuel dryness in many parts of the tropics (Dutra et al., 2022). The interaction between land-use pressures and climate variability has been shown to raise the risk of extreme fire events, particularly during warm phases of the El Niño–Southern Oscillation, as documented for the Bolivian Chiquitania, the southern Amazon, and other parts of the region (Devisscher et al., 2016; Dutra et al., 2022; Jakimow et al., 2023). These processes imply that fire cannot be treated solely as a natural hazard or a by-product of deforestation but needs to be analysed as an integral component of land-use change and forest degradation.

Against this backdrop, quantitative assessments of how fire activity relates to forest loss at national scales, and how these relationships interact with economic structure and institutional arrangements, remain relatively scarce. Global studies provide important context but aggregate across diverse regional drivers and policy regimes (Potapov et al., 2025; Tyukavina et al., 2015). National case studies, in turn, often focus either on specific fire events or on commodities, such as soy or cattle, without embedding their findings in a consistent, multi-country panel (Gibbs et al., 2015; Villoria et al., 2022; Heilmayr et al., 2020). Moreover, comparisons between satellite-based measurements of forest loss and national forest area statistics have highlighted inconsistencies and uncertainties that complicate the interpretation of deforestation trends, especially where degradation and temporary canopy removal are common (Li et al., 2017; Hansen et al., 2010; Egusa et al., 2020). In this paper, we use the term tree-cover loss to refer to the biophysical canopy change

detected by the Hansen Global Forest Change dataset (Hansen et al., 2013) and distinguish this from deforestation in the land-use sense, which implies a sustained change in land-use classification as captured by the FRA net forest area.

This study addresses that need by constructing a harmonized panel of annual tree cover loss, active fire detections, protected area status, FRA forest area, and macroeconomic indicators for twelve countries influenced by the Amazon basin during the period 2015-2023. Building on the Hansen Global Forest Change dataset, VIIRS active fire products, and FRA 2025 forest area statistics, the analysis quantifies the association between fire activity and tree-cover loss through a fixed-effects regression, examines the discrepancy between gross loss and net forest area change, and evaluates the share of loss occurring inside protected areas. By combining these elements, the study seeks to place regional fire-related forest loss in South America within the broader global context, while at the same time providing country-specific insights into how fire, economic composition, and governance interact.

The empirical results show that interannual variations in VIIRS fire detections on forest pixels are closely aligned with annual tree-cover loss in most countries, and that this relationship remains similar under alternative definitions of the fire metric and tree-cover threshold. The analysis also reveals substantial discrepancies between Hansen's gross loss and FRA net forest area change in several countries, suggesting that degradation and temporary disturbance contribute to forest cover dynamics beyond what is captured in land-use statistics. Furthermore, the study documents non-negligible loss inside protected areas, particularly in Venezuela, where other work has emphasized the role of mining and infrastructure within the Orinoco Mining Arc (Rivero & Liu, 2020; Rodriguez et al., 2021). These findings complement recent global assessments of fire-related forest disturbance by providing a regional perspective focused on the Amazon influence, and they underscore the importance of integrating satellite-based monitoring with national statistics and economic data when assessing progress toward forest and climate goals.

Because national reports under the 2030 Agenda for Sustainable Development use FRA-based indicators to track progress toward sustainable forest management and biodiversity conservation, discrepancies between satellite-derived tree-cover loss and FRA net forest area have implications for how countries are assessed against Sustainable Development Goals 13 (Climate Action) and 15 (Life on Land) (United Nations, 2015; United Nations, 2017). By examining where these data sources diverge and how fire activity contributes to that divergence, the present study is relevant for the interpretation of SDG indicators that rely on FRA statistics and for evaluations of the completeness of deforestation and degradation reporting in South America.

The remainder of the paper is structured as follows. The Methods section describes the construction of the panel dataset, including the treatment of Hansen Global Forest Change, VIIRS active fire detections, FRA forest area, protected areas, and socio-economic variables, as well as the specification of the fixed-effects regression. The Results section presents descriptive statistics and regression outcomes, including country-level summaries of loss and fire, the Hansen–FRA discrepancy ratio, protected-loss shares, and fire elasticity estimates. The Discussion section situates these findings within the existing literature on fire, deforestation, and forest monitoring, and examines methodological and policy implications. The Conclusion summarizes the main contributions and outlines directions for future research.

2. Materials and methods

2.1. Study area and temporal scope

The analysis focuses on twelve countries influenced by the Amazon basin and adjacent South American biomes: Argentina, Bolivia, Brazil, Chile, Colombia, Ecuador, Guyana, Paraguay, Peru, Suriname, Uruguay, and Venezuela. These countries cover a latitudinal range from the humid equatorial lowlands to subtropical and temperate forest systems. The study period spans the years 2015–2023, which corresponds to the interval where annual tree cover loss, active fire detections, and socio-economic indicators are jointly available and can be harmonized into a consistent panel.

All spatial statistics are calculated in the South America Albers Equal Area Conic projection (ESRI:102033). Equal-area projections are recommended for applications in which area is the quantity of interest and where the domain spans large latitude ranges, because conformal or geographic projections introduce systematic scale distortions that covary with latitude (e.g., Steinwand et al., 1995). Previous work on land-use and deforestation mapping for South America has demonstrated that area-preserving projections reduce bias in estimates of deforestation rates and change trajectories (e.g., Zalles et al., 2021). By using ESRI:102033 for all zonal computations, one hectare of forest loss in southern Chile is treated equivalently to one hectare in the equatorial Amazon.

2.2. Forest loss data

Forest disturbance is quantified using the Global Forest Change (GFC) dataset derived from Landsat imagery (Hansen et al., 2013). We use version 1.12 of the GFC product, which provides annual tree-cover loss from 2001 onwards at 30 m spatial resolution, together with tree-cover percentage in the year 2000, a datamask layer, and a binary gain layer. Following Hansen et al. (2013), "tree cover loss" is defined as a stand-replacement disturbance where canopy cover

decreases below 25 percent within the pixel footprint between successive annual composites. This definition does not distinguish between temporary canopy removal and permanent conversion.

We download all GFC tiles that intersect the South American continent and select four raster layers: the year of loss (lossyear), the baseline canopy cover in 2000 (treecover2000), a data validity mask (datamask), and a binary forest gain layer (gain). A tile discovery routine identifies all tiles with complete coverage in these layers and excludes tiles that are effectively oceanic. Two tiles south of the continent (30S_050W and 40S_060W) are excluded because the datamask indicates only water or no-data values and no land pixels intersect the study regions. A verification step confirms that all GFC tiles containing land pixels within the twelve study countries are included in the analysis and that no additional tiles bordering the study area were excluded due to missing or masked data. This procedure minimizes potential boundary effects in national loss estimates and ensures full spatial coverage of the study domain.

Forest loss is computed for three alternative canopy-cover thresholds: 10, 30, and 50 percent tree cover in the year 2000. For each GFC tile, the "treecover2000" layer is used to derive a binary mask of valid forest pixels for each threshold. The "datamask" layer is used to restrict calculations to pixels with valid observations. For every tile, loss year, and threshold, pixels with "lossyear" equal to the code of a given calendar year are identified within the valid forest mask. Each loss pixel is converted to area (hectares) by computing the area of each raster cell in the ESRI:102033 projection using the georeferencing transformation and summing across all pixels classified as loss. The use of an equal-area projection avoids latitude-dependent distortions in area calculations and ensures comparability of loss estimates across the wide latitudinal range of the study region.

The gain layer is used to compute a time-aggregated indicator of gross tree cover gain between 2000 and 2012 for each country, following the conventions of Hansen et al. (2013). Gain pixels are identified in the intersection of the datamask and regional polygons (see below), converted to area in hectares, and aggregated by country. Gain is not used as an explanatory variable in the panel regression; instead, it serves as a contextual indicator of the extent to which loss in the early 2000s may be offset by subsequent regrowth.

2.3. Administrative regions

All area statistics are computed at the national level. We use a regional boundary dataset that delineates the twelve target countries and is projected to ESRI:102033. These polygons are intersected with each GFC tile to obtain a per-tile union geometry. Only tiles that intersect at least one country's polygon are processed. Within each tile, the forest loss operations described above are performed separately for each country's polygon, ensuring that loss in border regions is attributed to the correct national territory.

Country codes are harmonized to ISO 3166-1 alpha-3 codes, and all intermediate summaries are stored using these identifiers. The final panel dataset thus contains, for each country and year, the total area of tree-cover loss at each canopy-cover threshold and the subset of loss that occurs inside protected areas (see next section).

2.4. Protected areas

Protected areas are represented using the World Database on Protected Areas (WDPA), November 2025 South America polygons. The WDPA database contains a large number of geometries with self-intersections, slivers, or other topological inconsistencies that can cause failures or silently incorrect results in overlay operations. Before any spatial analysis, we apply a geometry repair step using the `make_valid` operation provided by recent versions of the GEOS and Shapely libraries. The operation converts invalid geometries to valid polygon and multipolygon objects and separates geometry collections into simple features. We then recast the dataset to polygonal features only and discard non-polygon geometries.

To avoid look-ahead bias, only protected areas that were legally established before or during the first year of the analysis period are considered. The WDPA attribute "STATUS_YR" is cast to an integer, and features with "STATUS_YR" greater than 2015 are excluded. This ensures that the effective protected area network corresponds to the status at the beginning of the 2015–2023 period and that loss is not masked by protected areas that did not yet exist at the time of disturbance.

The cleaned WDPA polygons are reprojected to ESRI:102033. For each GFC tile, protected areas are intersected with the country boundaries to derive per-country protected area masks. When computing loss, we apply the same rasterization parameters as for the regional masks but use "all_touched=False" in the geometry mask, so that a pixel is assigned to a protected area only if its center lies within the polygon. This "center-pixel rule" reduces boundary overestimation and double counting across adjacent classes, which is particularly important for small or fragmented protected areas along national borders or rivers.

For every country, year, and canopy-cover threshold, we compute the total area of loss inside protected areas and express it both in hectares and as a share of total loss. This protected-loss share serves as an outcome indicator for the effectiveness of the protected area network in moderating tree-cover loss.

2.5. FRA forest area and net change

To relate remotely sensed tree-cover loss to official forest statistics, we use the Food and Agriculture Organization (FAO) Forest Resources Assessment (FRA) 2025 data set of country-level forest area by year. FRA forest area is derived from national forest inventories and administrative records and is based on land-use definitions rather than physical canopy cover. The FRA dataset used here provides forest areas for the years 1990, 2000, 2010, 2015, 2020, and 2025 for the twelve study countries.

FRA forest area statistics underpin several indicators used for national reporting on Sustainable Development Goal 15 and related forest targets, including measures of progress toward sustainable forest management (United Nations, 2015, 2017). Using the same underlying source in this study ensures that the discrepancies documented between satellite-derived loss and net forest area change are directly comparable to the information employed in official SDG monitoring. It should be noted that FRA forest area estimates originate from national forest inventories and administrative reporting systems and may therefore contain measurement uncertainty associated with sampling design, inventory updates, and definitional differences across countries. Because consistent uncertainty intervals are not reported for all national submissions, FRA values are treated as reported in the present analysis. Consequently, potential uncertainty in the original FRA estimates is assumed to remain constant over the interpolation interval and is not propagated through the discrepancy ratio calculations; the resulting comparisons should therefore be interpreted as indicative rather than strict statistical estimates of divergence between satellite-derived loss and official forest statistics

Because the panel analysis requires annual forest area and annual net change for 2015–2023, the coarsely spaced FRA series must be interpolated. We employ the Piecewise Cubic Hermite Interpolating Polynomial (PCHIP) method to generate annual values between the observed reporting years. PCHIP preserves monotonicity and avoids oscillatory behavior that can arise with classical cubic splines. When forest area declines between two FRA reporting years, PCHIP ensures that the interpolated series does not exhibit artificial intermediate increases, which would be implausible in the absence of large-scale restoration programs.

For each country, we construct a PCHIP interpolant using the FRA forest area reported for 1990, 2000, 2010, 2015, 2020, and 2025 and evaluate it for years 2015–2023. The annual values for 2015–2019 therefore lie between the 2015 and 2020 reports, and the values for 2021–2023 lie between the 2020 and 2025 reports. All years used in the panel thus fall within the 1990–2025 FRA reporting horizon, so the 2015–2023 series is obtained entirely by interpolation rather than extrapolation. For potential years beyond 2025, which are not analyzed in this study, a constant-value extrapolation would be used as a conservative "hold last value" strategy. The resulting series is expressed both in thousand hectares and in hectares. Annual net change is computed as the first difference of forest area by country; negative values represent net loss of forest area, whereas positive values indicate net gain or reclassification to forest land use.

These FRA time series are merged with the remotely sensed loss statistics to compute a discrepancy ratio between Hansen gross loss and FRA net forest area change. The ratio is defined only for years in which FRA net change is negative; in years with zero or positive net change, the ratio is left undefined because the denominator is zero or positive and the concept of "gross loss versus net loss" is not applicable.

2.6. Socio-economic indicators

To capture economic drivers of forest loss, we assemble annual data on gross domestic product (GDP) per capita in constant purchasing power parity terms and on the share of agriculture in value added. These series are taken from international databases as collated for an earlier version of the study and are available for 2000, 2010, and 2020. To derive values for intermediate years, we perform linear interpolation between the observed years and hold values constant beyond 2020, because no later observations are available.

For the regression analysis, GDP per capita is log-transformed, and the agriculture share is standardized to a z-score by subtracting its mean and dividing by its standard deviation within the panel. This transformation facilitates interpretation of coefficients and mitigates collinearity between level effects and country fixed effects.

2.7. VIIRS active fire detections

Fire activity is represented using the Visible Infrared Imaging Radiometer Suite (VIIRS) active fire product provided by the NASA Land Processes Distributed Active Archive Center. We use the SNPP VIIRS VNP14IMG product for the

years 2015–2023. All available country-level CSV files for the global archive are downloaded and filtered to the South American domain.

For each detection, we retain latitude, longitude, acquisition date and time, confidence category, and classification type. We restrict the analysis to detections within a bounding box that encompasses South America and to confidence categories labeled nominal or high. Detections classified as low confidence are excluded because they are associated with a higher probability of false positives, particularly in tropical environments where thermal anomalies may arise from non-fire sources such as sun glint, industrial heat sources, or mixed pixels containing warm surfaces. Restricting the analysis to nominal and high confidence detections follows common practice in regional analyses using VIIRS active fire products and improves the reliability of fire occurrence indicators used in statistical modelling (Schroeder et al., 2014; Giglio et al., 2016). Detections classified as static land sources or offshore are excluded, following common practice in satellite active fire assessments. Multiple detections with identical latitude, longitude, date, and time are removed to avoid exact duplicates.

The acquisition date is converted to a calendar year, and observations are restricted to the 2015–2023 period. Each detection is tagged with an ISO3 country code inferred from the file name and a tile key corresponding to the overlapping Hansen GFC tile. This tile key is derived from the center coordinates, aligned with the 10-degree grid of the GFC product.

Within each GFC tile, VIIRS points are raster-mapped to the GFC loss grid using the georeferencing transform, and only detections whose centers coincide with valid forest pixels (as defined by the datamask and tree-cover threshold) are retained. Two fire metrics are computed for each country, year, and threshold. The first metric, denoted “viirs_fire_count”, is the total number of fire detections on forest pixels in the current year and the preceding year, each weighted by 0.5. The second metric, “viirs_fire_unique_pxday”, applies an additional deduplication step: within each tile, detections are collapsed by pixel and day, so that multiple detections for the same pixel on the same day contribute only once. This deduplication procedure reduces repeated detections associated with persistent flaming fronts or multiple satellite overpasses and therefore provides a more conservative proxy for disturbance intensity.

Both fire metrics are aggregated from the tile level to the country level for each year and threshold. Because the mapping from detections to pixels is performed after the spatial subset to forest masks, detections in non-forest areas are automatically excluded. Throughout the analysis we therefore interpret the VIIRS-based variables as measures of aggregated fire detection intensity on forest pixels, not as counts of discrete fire events.

2.8. Panel construction and derived variables

All spatial and non-spatial components are merged into a country–year panel for the period 2015–2023. For each country, year, and canopy-cover threshold, the dataset contains GFC tree-cover loss in hectares, loss inside protected areas, VIIRS fire metrics, FRA forest area and net change, and socio-economic indicators. For the main regression analysis, we use the 30 percent canopy-cover threshold, which is widely applied in studies of tropical forest dynamics and represents a compromise between including open canopy formations and excluding sparsely wooded savannas.

The dependent variable in the regression is the natural logarithm of tree-cover loss plus one to accommodate zero values. The main explanatory variable of interest is the natural logarithm of the fire metric plus one. The primary specification uses the original “viirs_fire_count” metric; a parallel specification uses “viirs_fire_unique_pxday” to assess sensitivity to deduplication. The agriculture share is standardized, and log GDP per capita is included as a control. Country fixed effects are implemented via dummy variables. All variables are centered and scaled where appropriate to aid numerical stability.

In addition to the regression variables, the panel includes derived indicators used in descriptive analysis. The protected-loss share is the ratio of loss inside protected areas to total loss; it is used to summarize the relative importance of protected areas in moderating loss in each country. The discrepancy ratio, as defined above, is used to characterize differences between land-cover-based and land-use-based estimates of forest change.

2.9. Statistical analysis

The main statistical model is a linear panel regression with country fixed effects estimated via ordinary least squares. For a given fire metric and canopy-cover threshold, the model can be written in linear form as:

$$\log(\mathrm{Loss}_{i,t} + 1) = \beta_1 \times \log(\mathrm{Fire}_{i,t} + 1) + \beta_2 \times \mathrm{Z}\left(\mathrm{Agri}_{i,t}\right) + \beta_3 \times \log(\mathrm{GDP}_{i,t}) + \alpha_i + \varepsilon_{i,t}$$

where $\mathrm{Loss}_{i,t}$ is annual tree-cover loss in hectares for country i in year t, $\mathrm{Fire}_{\{it\}}$ is the fire metric, $\mathrm{Z}(\mathrm{Agri}_{i,t})$ is the standardized agriculture share, $\mathrm{GDP}_{i,t}$ is GDP per capita in constant purchasing power parity units, and alpha_i are country fixed effects. The coefficient beta_1 is interpreted as the elasticity of loss with respect to fire detections, and beta_2 as the percentage change in loss associated with a one-standard-deviation increase in the agriculture share.

Two variants of the model are estimated. Model 1 includes all three explanatory variables and the fixed effects. Model 2 excludes log GDP per capita to evaluate the sensitivity of the estimated fire and agriculture coefficients to the inclusion of this collinear control. We do not include year fixed effects in the main specification because the short time series and the strong co-movement of fire activity and loss during years such as 2016 would leave limited within-year variation for identifying the fire coefficient. Consequently, the estimated elasticity captures both the direct effect of fire detections and the component of continent-wide climatic conditions that come with fire and loss. Standard errors are computed under the assumption of homoscedastic disturbances; the small number of countries precludes reliable multi-way clustering, but alternative variance estimators can be explored in future work.

Multicollinearity is assessed by computing variance inflation factors for Model 1. As expected, the GDP variable exhibits high variance inflation due to its temporal smoothness and correlation with the fixed effects, whereas the fire and agriculture variables have more moderate values. Because dropping GDP from the specification does not materially alter the estimated fire coefficient, the interpretation of the fire–loss relationship is not driven by collinearity with GDP.

All statistical analysis is implemented in Python using the statsmodels library. Model outputs are summarized in a textual statistical appendix and graphically by plotting the relationship between fire metrics and loss, as well as the sensitivity of elasticity estimates across thresholds and fire metrics. These visual summaries are introduced in the Results section and referenced by figure number in the manuscript.

2.10. Code and data availability

To facilitate replication, all scripts and processed inputs used to construct the country–year panel and reproduce the figures are bundled in a dedicated replication package. The directory https://github.com/hresresearch/IMPLICATIONS-FOR-SDG-FOREST-MONITORING contains the full processing pipeline, including the preparation of regional boundaries and protected areas, the PCHIP interpolation of FRA forest area, the integration of Hansen loss, VIIRS fire detections, and socio-economic data, and the routines that generate all tables and figures. Script-level documentation is provided in both English and Spanish, and the package includes a requirements.txt file that specifies the Python environment used in the analysis. The complete replication package will be mirrored without modification in a public GitHub repository for long-term access.

3. Results

3.1. Nutrient removal assessment

The combined Hansen–FRA–VIIRS panel for the period 2015-2023 contains 108 observations per country-year for the twelve countries influenced by the Amazon and with a tree cover threshold of 30 percent. Over this period, the region experienced an aggregate tree-cover loss of approximately 45.2 million hectares. Brazil accounts for about two thirds of this total (29.5 million hectares), followed by Bolivia (4.5 million hectares), Paraguay (2.4 million hectares), Colombia (2.4 million hectares), and Peru (2.1 million hectares), whereas the Guiana Shield countries and Uruguay contribute comparatively small shares. Figure 2 summarizes the cumulative loss by country, and the main statistics are reported in Table 1.

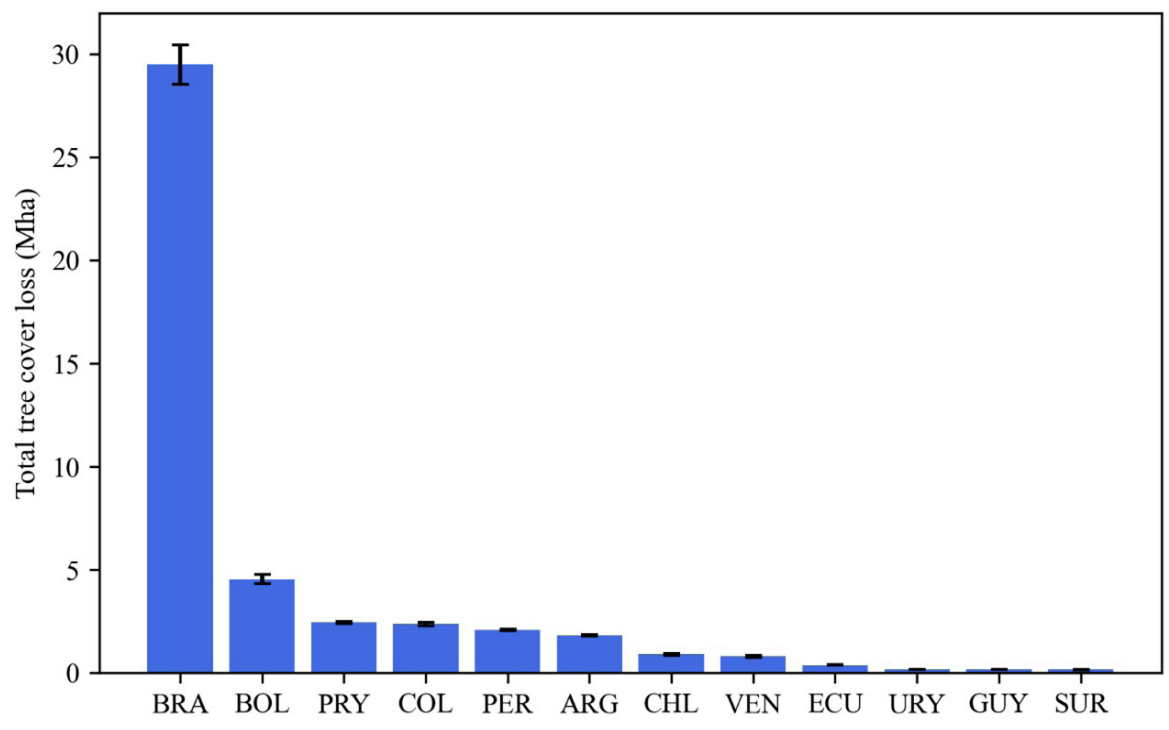

Figure 2. Cumulative gross tree-cover loss by country, 2015–2023, at a 30 percent canopy-cover threshold, aggregated from Hansen Global Forest Change.

Table 1. Summary of total tree-cover loss, average annual loss, mean discrepancy ratio, mean protected-loss share, and cumulative VIIRS fire detections by country for 2015–2023 (30 percent canopy-cover threshold).

Country (ISO3)	Total Hansen loss 2015–2023 (Mha)	Mean annual Hansen loss (kha)	Mean discrepancy ratio (Hansen/FRA)	Mean protected-loss share	Total VIIRS fire detections (millions)
ARG	1.80	200.38	1.09	0.02	0.58
BOL	4.54	504.75	2.39	0.10	1.54
BRA	29.51	3278.64	1.26	0.11	7.19
CHL	0.88	98.28	20.00	0.04	0.00
COL	2.36	262.60	1.77	0.05	0.40
ECU	0.37	41.33	0.81	0.02	0.04
GUY	0.15	17.13	2.03	0.01	0.02
PER	2.07	230.30	1.18	0.02	0.44
PRY	2.43	270.12	1.20	0.02	0.01
SUR	0.15	16.48	1.13	0.03	0.01
URY	0.16	18.13	Undefined	0.00	0.00
VEN	0.79	87.39	1.01	0.45	0.46

Annual loss trajectories differ across countries. Brazil exhibits both the largest absolute losses and pronounced interannual variability, including distinct peaks that correspond to the widely discussed fire years in the second half of the decade. Bolivia, Paraguay, and Peru show similar patterns of elevated loss during the late 2010s, whereas loss in Argentina and Chile is lower in magnitude and concentrated in years. The Guiana Shield countries retain relatively low annual loss levels throughout the period, in line with their classification as high-forest, low-deforestation jurisdictions in previous work (e.g., Teo et al., 2024). These temporal patterns are reflected in the yearly snapshots of loss and FRA net change presented in Table 2.

Table 2. Selected annual values of tree-cover loss, FRA net forest area change, and discrepancy ratio for key years (2016, 2019, 2023) by country at a 30 percent canopy-cover threshold.

Country (ISO3)	Year	Hansen loss (kha)	FRA net forest area change (kha)	Discrepancy ratio (Hansen/FRA)
ARG	2016	228.78	-208.74	1.10
ARG	2019	144.63	-180.16	0.80
ARG	2023	215.77	-179.55	1.20
BOL	2016	468.54	-199.73	2.35
BOL	2019	860.44	-235.57	3.65
BOL	2023	695.20	-239.83	2.90
BRA	2016	5242.97	-2319.72	2.26
BRA	2019	2645.04	-2782.76	0.95
BRA	2023	2748.56	-3264.08	0.84
CHL	2016	111.67	-2.33	47.95
CHL	2019	75.93	-8.07	9.41
CHL	2023	105.30	-4.90	21.48
COL	2016	268.14	-140.58	1.91
COL	2019	252.84	-181.86	1.39
COL	2023	179.45	-133.77	1.34
ECU	2016	40.25	-64.26	0.63
ECU	2019	34.96	-75.30	0.46
ECU	2023	39.42	-32.18	1.22
GUY	2016	25.93	-10.04	2.58
GUY	2019	21.89	-8.78	2.49
GUY	2023	27.20	-7.65	3.56
PER	2016	227.03	-201.15	1.13
PER	2019	226.48	-168.83	1.34
PER	2023	223.73	-302.93	0.74
PRY	2016	318.47	-286.57	1.11
PRY	2019	304.33	-232.83	1.31
PRY	2023	182.99	-165.90	1.10
SUR	2016	16.52	-9.55	1.73
SUR	2019	17.84	-17.17	1.04
SUR	2023	25.16	-18.30	1.37
URY	2016	23.76	21.78	Undefined

Country (ISO3)	Year	Hansen loss (kha)	FRA net forest area change (kha)	Discrepancy ratio (Hansen/FRA)
URY	2019	14.46	18.40	Undefined
URY	2023	20.85	18.40	Undefined
VEN	2016	171.29	-112.70	1.52
VEN	2019	118.55	-107.01	1.11
VEN	2023	60.93	-51.99	1.17

The comparison of Hansen's gross loss with FRA net forest area change indicates systematic differences between land-cover-based and land-use-based estimates. For years in which the FRA net change is negative, the discrepancy ratio covers a wide range, from values close to unity to values near 48 in extreme cases. Country-level averages show that Chile has a particularly high mean discrepancy ratio, close to 20, whereas Bolivia, Guyana, Colombia, and Brazil fall between about 1.3 and 2.4. In contrast, Ecuador and Venezuela display mean ratios close to or slightly below unity. Figure 3 shows the time series of the discrepancy ratio for all countries, ordered by magnitude. These results suggest that national forest statistics and remotely sensed estimates are closely aligned in some countries, while in others large areas of tree-cover loss are not reflected in net forest area change and therefore likely correspond to temporary disturbance or degradation processes.

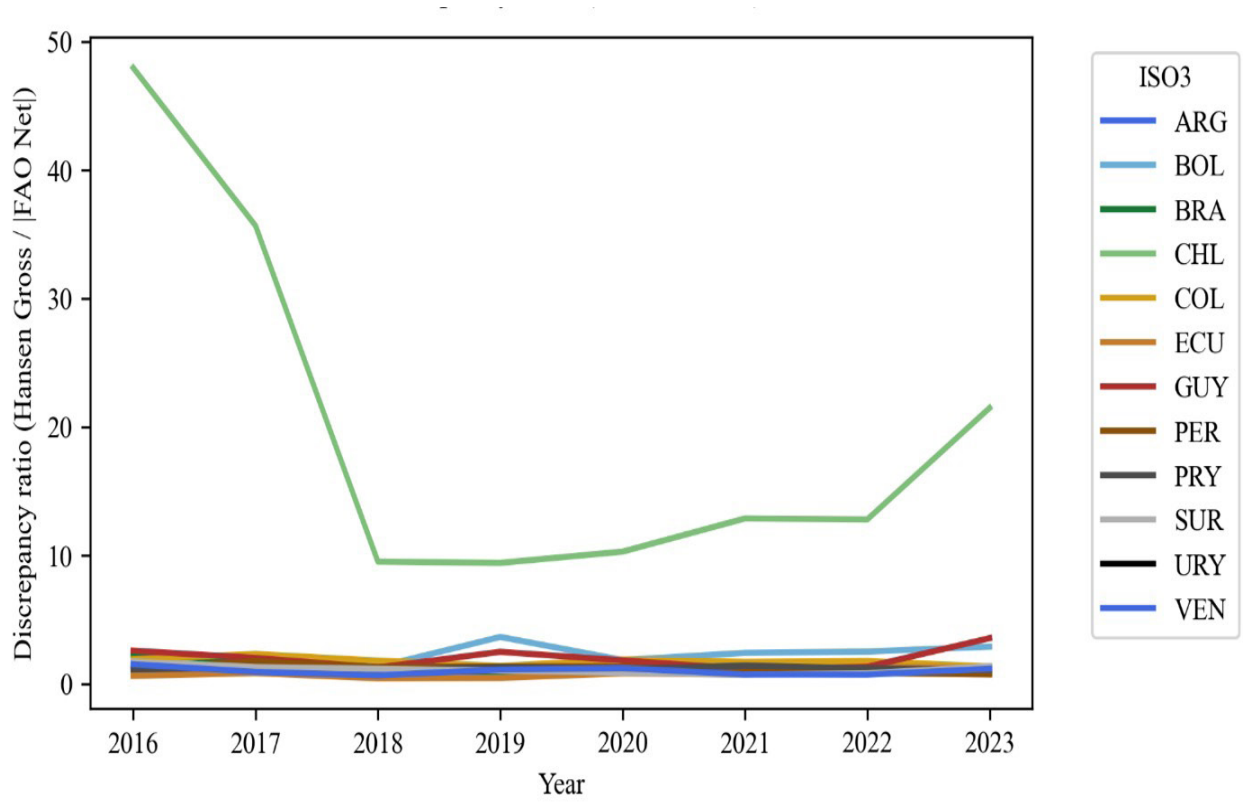

Figure 3. Time series of the Hansen–FRA discrepancy ratio for 2015–2023 by country at a 30 percent canopy-cover threshold, ordered by mean ratio.

Because the FRA forest area underlies indicators used for national reporting on Sustainable Development Goal 15, large discrepancy ratios imply that assessments of progress based solely on net forest area may overlook disturbance processes that are visible in satellite-based gross loss statistics (United Nations, 2015, 2017). In such cases, apparent stability or modest decline in official forest area can coincide with substantial fire-associated canopy removal, highlighting the value of considering both datasets jointly when interpreting SDG-related forest indicators.

The share of loss within protected areas also varies considerably across countries. Over 2015–2023, the mean protected-loss share is approximately 45 percent in Venezuela, indicating that nearly half of all tree-cover loss occurs inside legally designated protected areas. Brazil and Bolivia show mean values slightly above 10 percent, while Paraguay, Argentina, and Uruguay display values below 3 percent. The temporal evolution of protected-loss shares is summarized in Table 3, and the country means are visualized in Figure 4. These patterns are consistent with case-study reports that emphasize mining and infrastructure expansion inside Venezuelan protected areas (e.g., Lizarazo and García, 2020) and suggest that formal designation alone does not guarantee effective protection.

Table 3. Country-level mean and maximum protected-loss shares and the year of maximum protected-loss share during 2015–2023.

Country (ISO3)	Mean protected-loss share	Maximum protected-loss share	Year of maximum protected-loss share
ARG	0.017	0.049	2015
BOL	0.101	0.194	2020
BRA	0.106	0.127	2020
CHL	0.038	0.072	2020
COL	0.052	0.074	2018
ECU	0.024	0.030	2021
GUY	0.013	0.023	2022
PER	0.024	0.030	2017
PRY	0.022	0.061	2020
SUR	0.033	0.050	2016
URY	0.001	0.005	2018
VEN	0.453	0.574	2016

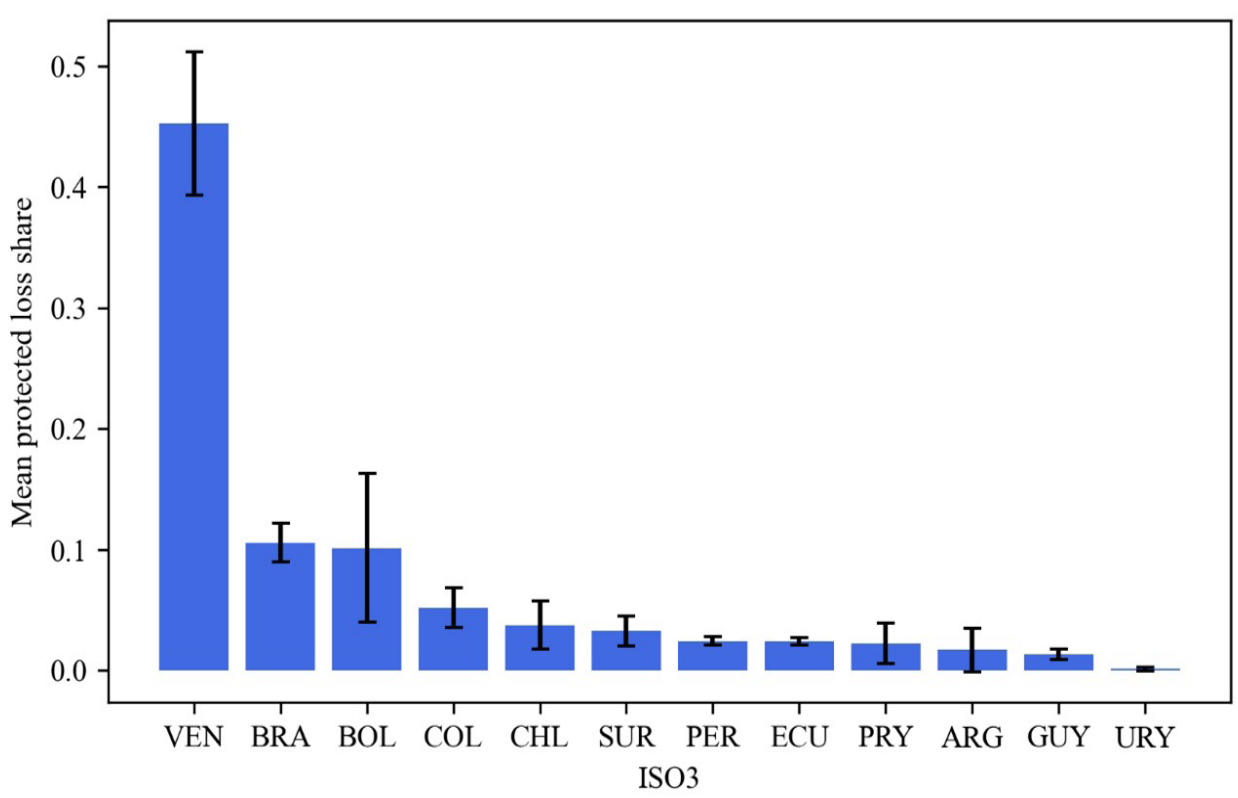

Figure 4. Mean share of tree-cover loss occurring inside protected areas for 2015–2023 by country at a 30 percent canopy-cover threshold.

The comparison between Hansen loss and VIIRS fire detections indicates a close association between fire activity and tree-cover loss at the country–year scale. The total number of forests-associated VIIRS detections is highest in Brazil (about 7.2 million detections over 2015–2023) and Bolivia (about 1.5 million), followed by Argentina, Venezuela, Peru, and Colombia. Scatter plots of annual Hansen loss against the weighted VIIRS fire count show that countries with higher fire activity generally experience greater loss, with Brazil and Bolivia occupying the upper end of both distributions (Figure 5).

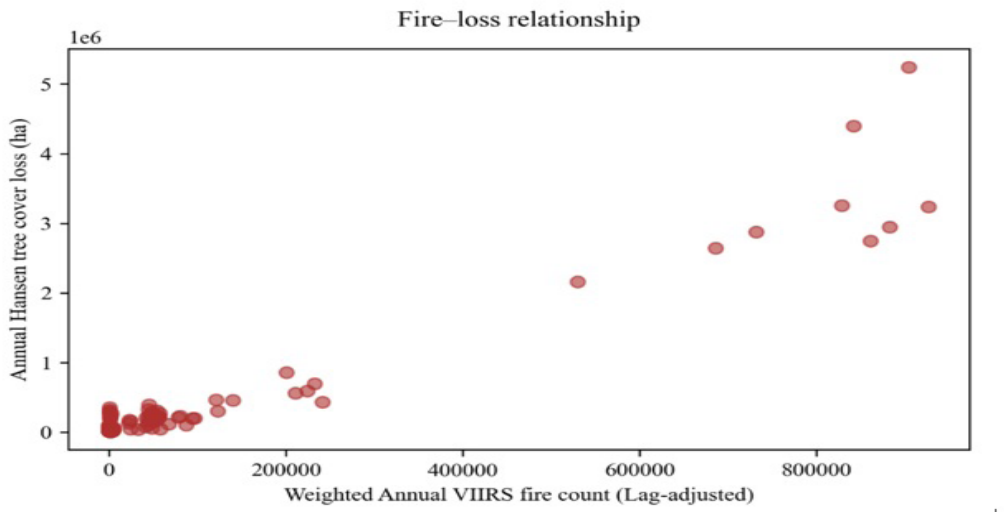

Figure 5. Relationship between weighted annual VIIRS fire detections and annual Hansen tree-cover loss by country and year at a 30 percent canopy-cover threshold, shown on linear and logarithmic scales.

Simple log–log regressions at the country level yield positive slopes in most cases, with especially steep slopes and high correlation coefficients in Brazil, Bolivia, Colombia, Guyana, and Peru. In contrast, countries with lower loss and fire activity, such as Uruguay and Paraguay, exhibit weak or inconsistent relationships. For Paraguay, the negative Pearson correlation likely reflects the fact that a substantial share of fire detections occurs in agricultural landscapes rather than forested areas, for example, during the burning of crop residues or pasture management. These fires may not coincide spatially or temporally with tree-cover loss detected in the Hansen dataset, leading to a weak or even negative association between annual fire detections and forest loss at the national scale.

The dual fire metrics allow an assessment of how sensitive the loss–fire relationship is to spatial and temporal deduplication of VIIRS detections. The ratio between the deduplicated metric based on unique pixel-day combinations and the original count metric has a mean value close to 1.0 across the panel, with a standard deviation of about 0.0003 and a minimum de around 0.998. Country-level means range from 0.9993 to 1.0. The scatterplot of the two metrics (Figure 6) shows that all country–year observations lie very close to the one-to-one line. This indicates that additional duplication has only a minor effect on the magnitude of the fire metric at the aggregation level used here and that the interpretation of fire as a proxy for disturbance intensity is not sensitive to this choice.

The fixed-effects regression analysis provides a more formal assessment of the association between fire detections, socio-economic drivers, and tree-cover loss. In the main specification, which uses the original weighted VIIRS fire count, the estimated coefficient on log fire is approximately 0.22 and statistically significant at conventional levels. In log–log form, this coefficient can be interpreted as an elasticity: a 1 percent increase in VIIRS fire detection intensity on forest pixels is associated with an increase of about 0.22 percent in annual tree-cover loss, holding constant country fixed effects, the standardized agriculture share, and log GDP per capita. The coefficient on the standardized agriculture share is positive and sizeable, implying that years in which agriculture contributes a larger-than-average share to value added tend to exhibit higher loss, although its statistical significance is marginal. GDP per capita does not attain statistical significance in any specification, and its inclusion or exclusion does not materially alter the estimated fire coefficient. The detailed regression output is summarized in a separate statistical appendix, while Table 4 reports simple fire–loss correlation diagnostics at the country level.

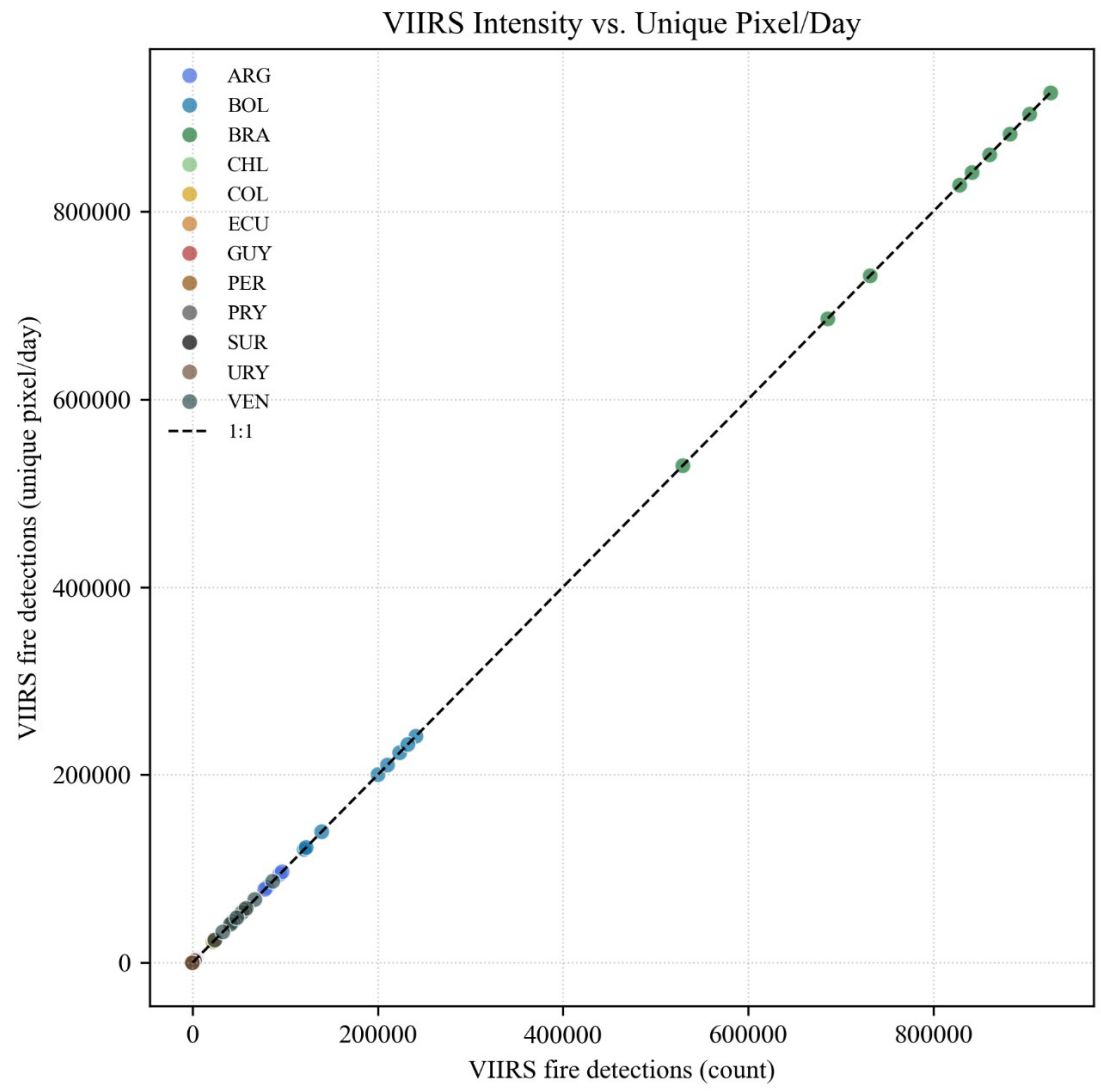

Figure 6. Comparison of weighted VIIRS fire detections and deduplicated unique pixel-day fire detections by country and year; the dashed line indicates the one-to-one relationship.

To examine sensitivity to the definition of the fire metric, an alternative specification replaces the original count metric with the unique pixel-day metric. The estimated elasticity of loss with respect to fire is nearly identical in magnitude and significance, consistent with the small differences between the two metrics at the descriptive level. Similarly, repeating the regression for the 10 and 50 percent canopy-cover thresholds yields fire coefficients that remain positive and of comparable size. Figure 7 summarizes the estimated fire elasticity across thresholds and fire metrics. Together with the descriptive results, these findings indicate that the strength and sign of the association between fire activity and tree-cover loss are not driven by the specific implementation of the VIIRS metric or the choice of canopy-cover threshold.

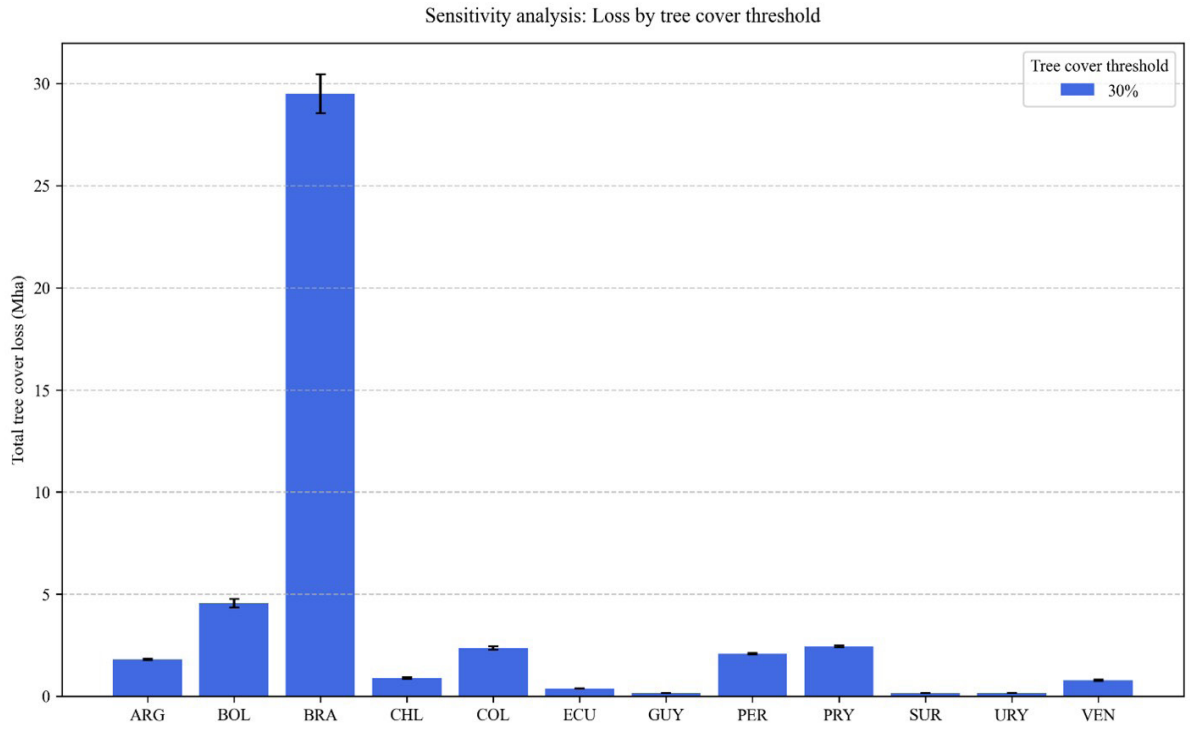

Figure 7. Estimated elasticity of annual tree-cover loss with respect to VIIRS fire detections across canopy-cover thresholds (10, 30, 50 percent) and fire metrics (weighted count and unique pixel-day), based on fixed-effects panel regressions.

Table 4. Pearson correlation coefficients and simple linear regression diagnostics (slope, intercept, p-value) relating annual Hansen tree-cover loss to weighted VIIRS fire detections by country.

Country (ISO3)	Pearson correlation (Hansen vs VIIRS)	Slope (ha per detection)	Intercept (ha)	p-value
ARG	0.35	0.44	172281.80	0.35
BOL	0.73	2.23	124092.40	0.03
BRA	0.60	4.48	-304396.00	0.09
CHL	0.70	421.96	75213.86	0.04
COL	0.57	4.94	41133.41	0.11
ECU	0.55	6.21	15063.92	0.12
GUY	0.81	5.42	3310.85	0.01
PER	0.64	2.34	116768.40	0.06
PRY	-0.34	-25.27	292937.20	0.37
SUR	0.61	5.00	9119.97	0.08
URY	0.15	67.02	17366.58	0.70
VEN	0.44	0.99	37126.25	0.24

The FRA interpolation check compares the PCHIP-interpolated forest area with a simple linear interpolation between FRA reporting years. For most countries, differences between the two methods are small, with mean absolute discrepancies in the range of a few hundred thousand hectares and maximum differences that are modest relative to national forest area. Brazil is an exception, as expected given its large forest area, but even in this case the differences do not alter the sign or broad magnitude of net forest area change. Table 5 reports these differences by country. The interpolation diagnostics support the use of PCHIP as a means of generating an annual forest area series that is smooth and monotone in periods of consistent decline, without introducing pronounced artifacts at the decadal boundaries.

Table 5. Maximum and mean absolute differences in FRA forest area between PCHIP and linear interpolation for 2015–2023 by country.

Country (ISO3)	Max absolute difference (kha)	Mean absolute difference (kha)
ARG	544.59	128.95
BOL	709.46	166.51
BRA	9375.50	2206.19
CHL	15.38	4.68
COL	419.77	102.01
ECU	111.29	29.69
GUY	23.80	5.79
PER	818.99	182.40
PRY	538.97	143.96
SUR	52.49	13.52
URY	55.85	13.34
VEN	178.25	49.32

Finally, the combination of Hansen loss, FRA net change, and VIIRS detections allows a qualitative comparison with recent global analyses of fire-related forest disturbance. Potapov et al. (2025) report that 2023 and 2024 have the highest global forest disturbance area due to fire since 2001 and that the share of fire-related disturbance has increased substantially, particularly in tropical regions. Although the panel in this study ends in 2023 and does not include 2024, the temporal patterns of loss and fire detections in Brazil, Bolivia, and other countries show elevated values toward the end of the period, consistent with an intensification of fire-related disturbance. The discrepancy ratios and protected-loss share further indicate that, in several countries, a substantial portion of fire-associated disturbance may not be reflected in net forest area statistics or may occur inside formally protected areas. These aspects are examined in more detail in the Discussion section.

4. Discussion

The results indicate that, over 2015–2023, fire activity measured by VIIRS detections is closely associated with annual tree-cover loss derived from Hansen Global Forest Change in the Amazon basin and adjacent South American biomes. The estimated elasticity of loss with respect to fire detections is around 0.22 across model variants and canopy-cover

thresholds, meaning that years with higher fire intensity tend to experience proportionally higher tree-cover loss. This pattern is consistent with broader evidence that the contribution of fire to forest disturbance has increased in recent decades, particularly in tropical regions (Potapov et al., 2025; Tyukavina et al., 2015). While the present analysis does not extend to 2024, the temporal concentration of loss and fire peaks in 2019–2020 in Brazil, Bolivia, and several neighboring countries mirrors the intensification of fire-related disturbance documented at the global scale.

The elasticity estimates suggest that fire is not merely a passive correlate of underlying land-use change but an important proximate driver of tree-cover loss in its own right. In several countries, such as Brazil, Bolivia, Colombia, Guyana, and Peru, log–log regressions at the country level show substantial slopes and high correlation coefficients between the fire metric and tree-cover loss. These relationships align with studies that have identified fire as a key mechanism in the transition from intact or selectively logged forests to open, degraded, or converted landscapes in the Amazon and Chaco regions (e.g., Devisscher et al., 2016; Zalles et al., 2021). In more densely populated agricultural frontiers, fires are often ignited intentionally for land clearing and pasture maintenance, and in years of anomalously dry conditions they escape into surrounding forests, amplifying loss beyond the area initially targeted (e.g., Dutra et al., 2022; Jakimow et al., 2023). The elasticity quantified in this study thus captures the integrated effect of both planned and unplanned fire use on forest cover in a regional panel framework.

At the same time, the estimated fire elasticity should be interpreted in the context of the measurement approach. The VIIRS metrics used here summarize the number of thermal anomalies detected on forest pixels and are therefore a proxy for fire activity rather than a direct measure of burned area or combustion completeness. The close alignment between the original weighted count and the deduplicated unique pixel-day metric implies that the intensity of detections at the country–year level is not highly sensitive to the handling of multiple detections over the same pixel. This is consistent with evaluations of VIIRS active fire products, which have shown that confidence filtering and conservative masking can yield stable measures of fire occurrence suitable for trend analysis. The analysis also confirms that, at the national scale considered here, the main inference about the association between fire and loss does not depend on whether repeated detections are treated as separate events or as indications of prolonged fire activity on the same pixel.

The positive coefficient of the standardized agriculture shares points to an additional dimension of the fire–loss relationship. Years in which agriculture accounts for a larger fraction of value added tend to have higher tree-cover loss, even after controlling for country fixed effects and fire activity. This finding is in line with the literature on commodity-driven deforestation in the Brazilian Amazon and surrounding regions, which links expansion of soy cultivation and pasture to increased forest loss and fire incidence (e.g., Moffette & Gibbs, 2021; Amaral et al., 2021). Supply-chain measures such as the Amazon Soy Moratorium have been shown to reduce direct conversion of primary forest to soy, but displacement of cattle ranching and crop expansion into previously cleared areas can still generate leakage effects and maintain high levels of fire use in frontier zones (Gibbs et al., 2015; Villoria et al., 2022; Heilmayr et al., 2020). The panel regression in this study does not disentangle specific commodities or land-use transitions, but the positive association between agriculture's economic weight and tree-cover loss is consistent with the broader evidence that market conditions and land-use incentives modulate the intensity of fire-mediated forest disturbance.

The discrepancy between gross tree-cover loss and net forest area change further contextualizes the role of fire and other drivers. The discrepancy ratio highlights that in several countries, notably Bolivia, Paraguay, Guyana, and Colombia, remotely sensed gross loss substantially exceeds the net forest area change reported to the FAO. Similar divergences between satellite-based forest area estimates and national inventories have been documented in other regions and periods (e.g., Li et al., 2017; Hansen et al., 2010). The reasons typically include differences in forest definitions, treatment of temporary disturbance, minimum mapping units, and the handling of plantations and non-forest tree cover. In Chile, for example, the very high average discrepancy ratio likely reflects the importance of industrial plantations and rotation forestry, where repeated clear-cuts appear as tree-cover loss in Hansen but may not be reported as net forest area loss in FRA if the land remains within the forest land use category. In contrast, near-unity ratios in Brazil and Ecuador suggest closer alignment between remote sensing and FRA statistics, possibly due to long-running national monitoring systems and more consistent definitions across data sources.

The presence of large discrepancy ratios in several countries has implications for both carbon accounting and policy evaluation. If gross tree-cover loss linked to fire or logging is not reflected in net forest area change, national greenhouse gas inventories may underestimate emissions from degradation and foregone carbon sequestration (Baccini et al., 2017; Li et al., 2017; Egusa et al., 2020). Studies comparing national inventory-based estimates with satellite-derived biomass and disturbance products have emphasized that omission of degradation processes can bias assessments of progress toward climate and forest goals. The discrepancy ratio operationalized in this study does not resolve all definitional issues but provides a simple indicator of where such underestimation is likely and where further reconciliation between data sources is needed. In Bolivia, for instance, the combination of high discrepancy ratios and elevated fire-related loss

is consistent with reports that large areas burned during the 2019 Chiquitania fires were not fully captured in official deforestation statistics (Devisscher et al., 2016).

The analysis of protected-loss shares reveals another dimension of the gap between formal classifications and on-the-ground outcomes. The finding that nearly half of all tree-cover loss in Venezuela occurs inside protected areas aligns with case-based studies of the Orinoco Mining Arc, which document extensive mining, road construction, and settlement expansion within areas formally designated for conservation or Indigenous use (Rivero & Liu, 2020; Rodriguez et al., 2021). Rather than suggesting that protected area status itself is inappropriate, this pattern points to governance challenges related to limited enforcement capacity and strong economic incentives for resource extraction in forest frontier regions. Where large-scale mining or infrastructure projects overlap with conservation areas, protected status may coexist with significant forest disturbance when monitoring and enforcement are weak.

From a policy perspective, these findings highlight the importance of strengthening institutional capacity for monitoring and enforcement, while also aligning conservation policies with broader economic and land-use governance frameworks. Similar mining-related forest disturbance has been documented elsewhere in the Amazon and the Guiana Shield, where extractive activities generate forest loss inside or near protected landscapes despite high overall forest cover (Sonter et al., 2017; Dezécache et al., 2017; Roopsind et al., 2019).

Similar patterns of mining-related deforestation have been observed in parts of the Brazilian Amazon, where industrial mining and associated infrastructure can cause substantial forest loss both inside and near protected areas (Sonter et al., 2017), and in the Guiana Shield, where gold mining drives forest degradation in jurisdictions that otherwise maintain high overall forest cover (Dezécache et al., 2017; Roopsind et al., 2019). The protected-loss indicators presented here are coarse and do not distinguish between different categories of protection or governance regimes, but they underscore that the legal status of land is not a reliable proxy for effective protection against fire-mediated disturbance and conversion.

Methodological choices in the geospatial processing pipeline also deserve discussion in light of existing literature. The decision to conduct all area calculations in an equal-area projection, and specifically ESRI:102033, is consistent with recommendations from comparative studies of map projections for global and continental data sets (Steinwand et al., 1995). These studies show that preserving area is relevant when aggregating pixel-based quantities over large extents, because non-equal-area projections can produce latitude-dependent distortions that accumulate in regional summaries. Similarly, the use of the "center-pixel rule" ("all_touched=False") when rasterizing region and protected-area masks is motivated by analyses of pixel overlap and boundary effects in raster GIS, which demonstrate that including all touched pixels can systematically overestimate area in narrow or fragmented features. The present results confirm that, with these safeguards, per-country loss estimates behave in a manner consistent with published deforestation statistics and avoid artificial inflation at region boundaries.

The treatment of the FRA forest area is another methodological aspect with implications for interpretation. Interpolating the FRA forest area between reporting years is unavoidable when annual net change is required, but the choice of interpolation method affects the inferred trajectory. By using PCHIP interpolation on the FRA forest area reported for 1990, 2000, 2010, 2015, 2020, and 2025, the present analysis ensures that annual values for 2015–2023 are obtained entirely by interpolation within the observed 1990–2025 FRA horizon rather than by extrapolation beyond it. This approach avoids artifacts associated with both linear interpolation and higher-order splines: declines in forest area remain monotone between successive FRA reports, and the post-2025 evolution of FRA forest area is treated as unknown rather than projected. The diagnostics in Table 5, which compare PCHIP with a linear alternative, indicate that differences are modest relative to national forest areas and do not change the broad conclusions about the sign and magnitude of net forest change in the period of interest. We also verified that all Hansen GFC tiles that contain land pixels within the twelve study countries are present and contain complete lossyear and datamask layers; two additional tiles located south of the continent (30S_050W and 40S_060W) consist entirely of no-data values and are therefore excluded from the analysis. Incomplete tile coverage is thus unlikely to bias the national loss aggregates.

The combination of Hansen loss and VIIRS detections with FRA and socio-economic data yields a coherent picture of how fire, land-use dynamics, and institutional settings interact in this region. The dominance of Brazil and Bolivia in both fire detections and tree-cover loss, together with elevated discrepancy ratios and protected-loss shares in several countries, is consistent with previous findings that commodity expansion, infrastructure, and extractive industries have extended deforestation and degradation into new frontiers (Zalles et al., 2021; Sonter et al., 2017). At the same time, the relatively low loss and moderate discrepancy ratios in the Guiana Shield are in line with analyses of high-forest, low-deforestation jurisdictions, which emphasize the importance of governance choices and economic structure in maintaining low deforestation despite external pressures (Teo et al., 2024; Roopsind et al., 2019). The panel perspective of this study contributes to this literature by quantifying how annual variations in fire activity and economic composition are reflected in tree-cover loss within individual countries.

Several limitations of the present analysis should be considered when interpreting the results. First, the study period ends in 2023 and therefore does not cover the record 2024 fire season documented by Potapov et al. (2025). As a result, the panel does not capture the most recent acceleration of fire-related disturbance in some climate domains. Second, the analysis is conducted at the national level, which masks sub-national heterogeneity in drivers and responses; sub-national panels that distinguish biomes, states, or municipalities would be needed to study local policy effects or frontier dynamics in more detail (Dutra et al., 2022).

Third, the fire metrics are based on active fire detections rather than burned areas. VIIRS identifies thermal anomalies associated with actively burning pixels but does not measure the spatial extent of burned areas. As a result, some fires, particularly low-intensity understory fires occurring beneath dense forest canopies, may be less detectable than fires associated with open clearing or agricultural burning. This detection bias may affect the interpretation of the estimated fire–loss elasticity, especially in densely forested regions where understory fires contribute to degradation without necessarily producing strong thermal signals detectable by satellite sensors. The regression also does not include explicit climate variables such as vapor pressure deficit or fire weather indices, which have been shown to influence fire occurrence and spread (Dutra et al., 2022).

Because the panel specification includes country fixed effects but no explicit year fixed effects, continent-wide climatic shocks, such as strong El Niño events, may influence both fire activity and tree-cover loss simultaneously. In such cases, part of the variation associated with these climatic conditions may be captured by the fire variable itself. The estimated elasticity should therefore be interpreted as reflecting the combined influence of fire detections and broader climatic conditions that increase fire probability and forest disturbance during anomalously dry years. Finally, the socio-economic data are limited to GDP per capita and agriculture's share of value added, which are coarse proxies for the range of land-use and governance factors that influence forest outcomes.

The findings also have implications for the interpretation of Sustainable Development Goal indicators that rely on FRA statistics. FRA-based metrics used for SDG 15 reporting summarize net forest area change at the national scale (United Nations, 2017). Where discrepancy ratios are large and fire-related disturbance is substantial, gross tree-cover loss and associated carbon fluxes can exceed what is implied by net area change alone, particularly when temporary canopy removal and degradation are classified as remaining forest land. In such settings, integrating satellite-based gross loss and active fire data with FRA reporting can provide complementary information for assessing progress toward SDG 13 and SDG 15 and for identifying cases in which apparent stability in net forest area masks increasing disturbance pressure.

Despite these limitations, the analysis provides quantitative evidence that aligns with and complements recent global studies of fire-related forest disturbance. It confirms that, in the Amazon basin and adjacent South American biomes, fire activity measured by VIIRS is closely tied to tree-cover loss and that this association persists after accounting for economic context and cross-country heterogeneity. It further demonstrates that official forest area statistics may understate the extent of disturbance in some countries, particularly where degradation and temporary canopy removal play a large role, and that protected-area designations do not necessarily prevent fire-related loss. These findings underscore the importance of integrating satellite-based disturbance and fire data with national inventories and socio-economic information when assessing progress toward forest and climate targets. The next section examines the implications of these findings for conservation policy, monitoring, and future research.

5. Conclusions

This study combined satellite-derived tree-cover loss, active fire detections, protected-area boundaries, FAO forest statistics, and socio-economic indicators to examine how fire and economic drivers relate to annual forest loss in the Amazon basin and adjacent South American biomes between 2015 and 2023. By integrating Hansen Global Forest Change with VIIRS active fire data and FRA forest area, and by estimating a fixed-effects panel regression, the analysis provides a consistent picture of how interannual fire activity and economic structure are reflected in national-scale tree-cover loss.

Three main conclusions emerge. First, fire activity detected by VIIRS on forest pixels is closely associated with annual tree-cover loss at the country–year level. The estimated elasticity of loss with respect to fire detections is approximately 0.22 across specifications and canopy-cover thresholds, indicating that relative changes in fire intensity are mirrored by proportionally smaller but meaningful changes in loss. This relationship persists after controlling for country fixed effects and macro-economic variables and is stable when a deduplicated fire metric based on unique pixel-day combinations is used instead of the original weighted count. In combination with recent global analyses of fire-related disturbance, these results reinforce the view that fire has become a central proximate driver of forest disturbance in tropical South America during the past decade.

Second, the comparison between Hansen gross tree-cover loss and FRA net forest area change reveals systematic discrepancies that are informative about degradation processes and reporting practices. In several countries, notably Bolivia, Paraguay, Guyana, and Colombia, remotely sensed gross loss substantially exceeds net forest area change, implying that large areas of canopy removal are not classified as permanent deforestation in land-use statistics. In Chile, the very high discrepancy ratios likely reflect rotation forestry and plantation dynamics, whereas near-unity ratios in Brazil and Ecuador suggest closer alignment between satellite products and national reporting. The discrepancy ratio used in this study is intentionally simple, but it provides an operational indicator of where degradation and temporary disturbance are likely underrepresented in official statistics. This has direct implications for carbon accounting and for the evaluation of progress toward forest and climate targets, because emissions from degradation and foregone removals can be substantial even when net forest area appears stable.

Third, the analysis of loss inside protected areas and the association with agricultural activity underscores the importance of governance and economic context. The finding that nearly half of all tree-cover loss in Venezuela occurs within protected areas is consistent with reports of mining and infrastructure expansion inside the Orinoco Mining Arc and indicates that formal protection alone is insufficient to prevent forest disturbance. In Brazil, Bolivia, and several other countries, non-trivial protected-loss shares coexist with clear fire–loss relationships and a positive association between the agricultural share of value added and tree-cover loss. These patterns align with the literature on commodity-driven deforestation and suggest that policies targeting specific sectors and frontiers are needed to moderate fire-mediated loss, even where broad conservation frameworks and supply-chain initiatives are in place.

Methodologically, the study demonstrates that careful choices in projection, masking, interpolation, and fire metric construction can reduce several sources of bias that have been discussed in the literature. The use of an equal-area projection and the center-pixel rule mitigate area distortion and boundary overestimation; PCHIP interpolation of FRA forest area avoids artificial oscillations in annual net change; and the dual VIIRS metrics show that conclusions about the fire–loss relationship are not an artifact of multiple detections over the same pixel. The combination of these elements yields a panel dataset and analytical framework that can be extended to additional years and regions as new data become available.

Several limitations remain. The panel does not include the record 2024 fire season highlighted by Potapov et al. (2025), and the national aggregation hides sub-national heterogeneity in drivers and policies. The regression does not explicitly incorporate climate variables or detailed land-use data, and the socio-economic indicators are limited to GDP per capita and the agricultural share of value added. Future work could extend the analysis by adding burned-area products, climate indices, and commodity-specific land-use information; by estimating sub-national panels that distinguish biomes and administrative units; and by integrating intact forest landscape data to more directly assess impacts on high-biomass forests.

Despite these limitations, the findings support three broad policy messages. Monitoring systems and mitigation strategies that address fire dynamics are essential for managing forest loss in tropical South America, as policies that focus solely on deforestation may overlook an important driver of forest disturbance. Improving the consistency between satellite-based observations and national forest statistics is important for transparent reporting and for aligning national inventories with independent monitoring systems. A practical step would be to complement SDG forest indicators based on net forest area change with satellite-derived metrics of gross tree-cover loss and disturbance frequency, allowing monitoring frameworks to capture both permanent land-use change and temporary canopy disturbances that may not be reflected in official forest statistics.

Strengthening governance in protected areas and frontier regions remains relevant for limiting fire-mediated forest disturbance, particularly in countries where a substantial share of loss occurs within protected boundaries. This includes improving enforcement against illegal mining, land speculation, and other extractive activities that can drive forest degradation even within formally protected landscapes. By linking fire detections, tree-cover loss, and national forest statistics in a consistent analytical framework, this study contributes to the evidence base needed to support more integrated forest monitoring systems and to inform assessments of progress toward Sustainable Development Goals 13 (Climate Action) and 15 (Life on Land) in South America.

Conflict of Interest

The authors declare that they have no conflict of interest.

Declaration of competing interests

The authors affirm that there are no conflicts of interest to disclose.

References

Achard, F., Eva, H., Stibig, H.-J., Mayaux, P., Gallego, J., Richards, T., & Malingreau, J.-P. (2002). Determination of deforestation rates of the world's humid tropical forests. *Science*. https://doi.org/10.1126/SCIENCE.1070656

Amaral, D. F., de Souza Ferreira Filho, J. B., Chagas, A. L. S., & Adami, M. (2021). Expansion of soybean farming into deforested areas in the Amazon biome: The role and impact of the Soy Moratorium. *Sustainability Science*. https://doi.org/10.1007/S11625-021-00942-X

Baccini, A., Walker, W. S., Carvalho, L., Farina, M., Sulla-Menashe, D., & Houghton, R. A. (2017). Tropical forests are a net carbon source based on aboveground measurements of gain and loss. *Science*. https://doi.org/10.1126/SCIENCE.AAM5962

Devisscher, T., Anderson, L. O., Aragão, L. E. O. C., Guerrero Galván, L. R., & Malhi, Y. (2016). Increased wildfire risk driven by climate and development interactions in the Bolivian Chiquitania, Southern Amazonia. *PLOS ONE*. https://doi.org/10.1371/JOURNAL.PONE.0161323

Dutra, D. J., Anderson, L. O., Fearnside, P. M., Graça, P. M. L. A., Yanai, A. M., Dalagnol, R., Burton, C., Jones, C., Betts, R., & Aragão, L. E. O. C. (2022). Fire dynamics in an emerging deforestation frontier in southwestern Amazonia, Brazil. *Fire*. https://doi.org/10.3390/FIRE6010002

Egusa, T., Kumagai, T., & Shiraishi, N. (2020). Carbon stock in Japanese forests has been greatly underestimated. *Scientific Reports*. https://doi.org/10.1038/S41598-020-64851-2

Gibbs, H. K., Rausch, L., Munger, J., Schelly, I., Morton, D. C., Noojipady, P., Soares-Filho, B., Barreto, P., Micol, L., & Walker, N. F. (2015). Brazil's Soy Moratorium. *Science*. https://doi.org/10.1126/SCIENCE.AAA0181

Hansen, M. C., Potapov, P., Moore, R., Hancher, M., Turubanova, S., Tyukavina, A., Thau, D., Stehman, S. V., Goetz, S. J., Loveland, T. R., Kommareddy, A., Egorov, A, Chini, L., Justice, C. O., & Townshend, J. R. (2013). High-resolution global maps of 21st-century forest cover change. *Science*. https://doi.org/10.1126/SCIENCE.1244693

Hansen, M. C., Stehman, S. V., & Potapov, P. (2010). Quantification of global gross forest cover loss. Proceedings of the National Academy of Sciences of the United States of America. https://doi.org/10.1073/PNAS.0912668107

Heilmayr, R., Rausch, L., Munger, J., & Gibbs, H. K. (2020). Brazil's Amazon Soy Moratorium reduced deforestation. *Nature Food*. https://doi.org/10.1038/S43016-020-00194-5

Jakimow, B., Baumann, M., de Souza Cruz Salomão, C., Bendini, H. N., & Hostert, P. (2023). Deforestation and agricultural fires in South-West Pará, Brazil, under political changes from 2014 to 2020. *Journal of Land Use Science*. https://doi.org/10.1080/1747423X.2023.2195420

Li, Y., Li, Y., Sulla-Menashe, D., Motesharrei, S., Song, X.-P., Kalnay, E., Ying, Q., Li, S., & Ma, Z. (2017). Inconsistent estimates of forest cover change in China between 2000 and 2013 from multiple datasets: Differences in parameters, spatial resolution, and definitions. *Scientific Reports*. https://doi.org/10.1038/S41598-017-07732-5

Maxwell, S. L., Evans, T., Watson, J. E. M., Morel, A. C., Grantham, H. S., Duncan, A., Harris, N. L., Potapov, P., Runting, R. K., Venter, O., Wang, S., & Malhi, Y. (2019). Degradation and forgone removals increase the carbon impact of intact forest loss. *Science Advances*. https://doi.org/10.1126/SCIADV.AAX2546

Moffette, F., & Gibbs, H. K. (2021). Agricultural displacement and deforestation leakage in the Brazilian Legal Amazon. *Land Economics*. https://doi.org/10.3368/WPLE.97.1.040219-0045R

Potapov, P., Tyukavina, A., Turubanova, S., Hansen, M. C., Giglio, L., Hernandez-Serna, A., Lima, A., Harris, N., & Stolle, F. (2025). Unprecedentedly high global forest disturbance due to fire in 2023 and 2024. Proceedings of the National Academy of Sciences, 122(30), e2505418122. https://doi.org/10.1073/pnas.2505418122

Rivero, D., & Liu, Y. (2020). Venezuela's Orinoco Mining Arc: A literature review of environmental impacts. International *Journal of Scientific and Research Publications*. https://doi.org/10.29322/IJSRP.10.02.2020.P9812

Rodriguez, E. A. T., Michinaux, A. A., & Awomuti, A. (2021). Environmental impact assessment and the controversy of the mining arc in Venezuela. *International Journal of Scientific and Research Publications*. https://doi.org/10.29322/IJSRP.11.04.2021.P11256

Roopsind, A., Sohngen, B., & Brandt, J. S. (2019). Evidence that a national REDD+ program reduces tree cover loss and carbon emissions in a high forest cover, low deforestation country. Proceedings of the National Academy of Sciences of the United States of America https://doi.org/10.1073/PNAS.1904027116

Sonter, L. J., Herrera, D. A., Barrett, D., Galford, G. L., Moran, C., & Soares-Filho, B. (2017). Mining drives extensive deforestation in the Brazilian Amazon. *Nature Communications*. https://doi.org/10.1038/S41467-017-00557-W

Steinwand, D. R., Hutchinson, J. A., & Snyder, J. P. (1995). Map projections for global and continental data sets and an analysis of pixel distortion caused by reprojection. *Photogrammetric Engineering and Remote Sensing*. https://pubs.usgs.gov/publication/70187049

Teo, H. C., Sarira, T. V., Tan, A. R. P., Cheng, Y.-B., & Koh, L. P. (2024). Charting the future of high forest low deforestation jurisdictions. Proceedings of the National Academy of Sciences of the United States of America. https://doi.org/10.1073/pnas.2306496121

Tyukavina, A., Baccini, A., Hansen, M. C., Potapov, P., Stehman, S. V., Houghton, R. A., Krylov, A., Turubanova, S., & Goetz, S.J. (2015). Aboveground carbon loss in natural and managed tropical forests from 2000 to 2012. *Environmental Research Letters*. https://doi.org/10.1088/1748-9326/10/7/074002

United Nations. (2015). Transforming our world: The 2030 Agenda for Sustainable Development (A/RES/70/1). United Nations. https://sdgs.un.org/2030agenda

United Nations. (2017). Global indicator framework for the Sustainable Development Goals and targets of the 2030 Agenda for Sustainable Development (A/RES/71/313). United Nations. https://unstats.un.org/sdgs/indicators/Global%20Indicator%20Framework%20after%202022%20refinement_Eng.pdf

Villoria, N. B., Garrett, R. D., Gollnow, F., & Carlson, K. M. (2022). Leakage does not fully offset soy supply-chain efforts to reduce deforestation in Brazil. *Nature Communications*. https://doi.org/10.1038/s41467-022-33213-z

Zalles, V., Hansen, M. C., Potapov, P., Parker, D., Stehman, S. V., Pickens, A. H., Parente, L., Ferreira, L. G., Song, X.-P., Hernandez-Serna, A., & Kommareddy, I. (2021). Rapid expansion of human impact on natural land in South America since 1985. *Science Advances*. https://doi.org/10.1126/SCIADV.ABG1620